Article

Reconstruction of Insulin Signal Flow
from Phosphoproteome and Metabolome Data

Katsuyuki Yugi,[1,9] Hiroyuki Kubota,[1,7,8,9] Yu Toyoshima,[1] Rei Noguchi,[2] Kentaro Kawata,[1] Yasunori Komori,[1] Shinsuke Uda,[1,7] Katsuyuki Kunida,[1] Yoko Tomizawa,[1] Yosuke Funato,[3] Hiroaki Miki,[3] Masaki Matsumoto,[4] Keiichi I. Nakayama,[4] Kasumi Kashikura,[5] Keiko Endo,[5] Kazutaka Ikeda,[5] Tomoyoshi Soga,[5] and Shinya Kuroda[1,2,6,*]

[1]Department of Biological Sciences, Graduate School of Science
[2]Department of Computational Biology, Graduate School of Frontier Sciences
University of Tokyo, Hongo 7-3-1, Bunkyo-ku, Tokyo 113-0033, Japan
[3]Department of Cellular Regulation, Research Institute for Microbial Diseases, Osaka University, Suita, Osaka 565-0871, Japan
[4]Department of Molecular and Cellular Biology, Medical Institute of Bioregulation, Kyushu University, 3-1-1 Maidashi, Higashi-ku, Fukuoka, Fukuoka 812–8582, Japan
[5]Institute for Advanced Biosciences, Keio University, Tsuruoka, Yamagata 997-0052, Japan
[6]CREST, Japan Science and Technology Corporation, Bunkyo-ku, Tokyo 113-0033, Japan
[7]Division of integrated Omics, Research Center for Transomics Medicine, Medical Institute of Bioregulation, Kyushu University, 3-1-1 Maidashi, Higashi-ku, Fukuoka, Fukuoka 812-8582, Japan
[8]PRESTO, Japan Science and Technology Corporation, Higashi-ku, Fukuoka, Fukuoka 812-8582, Japan
[9]Co-first author
*Correspondence: skuroda@bs.s.u-tokyo.ac.jp
http://dx.doi.org/10.1016/j.celrep.2014.07.021
This is an open access article under the CC BY license (http://creativecommons.org/licenses/by/3.0/).

SUMMARY

Cellular homeostasis is regulated by signals through multiple molecular networks that include protein phosphorylation and metabolites. However, where and when the signal flows through a network and regulates homeostasis has not been explored. We have developed a reconstruction method for the signal flow based on time-course phosphoproteome and metabolome data, using multiple databases, and have applied it to acute action of insulin, an important hormone for metabolic homeostasis. An insulin signal flows through a network, through signaling pathways that involve 13 protein kinases, 26 phosphorylated metabolic enzymes, and 35 allosteric effectors, resulting in quantitative changes in 44 metabolites. Analysis of the network reveals that insulin induces phosphorylation and activation of liver-type phosphofructokinase 1, thereby controlling a key reaction in glycolysis. We thus provide a versatile method of reconstruction of signal flow through the network using phosphoproteome and metabolome data.

INTRODUCTION

Cellular homeostasis is dynamically regulated by signals that are transmitted in global multiple molecular ("trans-omic") networks that include proteins and their phosphorylation, mRNAs, and metabolites (Brazhnik et al., 2002; Buescher et al., 2012; Feist et al., 2009; Gerosa and Sauer, 2011; Güell et al., 2009; Ishii et al., 2007; Joyce and Palsson, 2006; Kühner et al., 2009; Locasale et al., 2011; Oliveira et al., 2012; Shyh-Chang et al., 2013; Vander Heiden et al., 2010; Yus et al., 2009). To understand the mechanism of cellular homeostasis, we introduce here the concept of signal flow. Signal flow consists of static signal flow and dynamic signal flow. Static signal flow is the route of the signal in a trans-omic network. Dynamic signal flow is the traffic of the signal, or the temporal changes in molecular concentrations that are transmitted through the route. Thus, traffic and routes illustrate when and where signals flow in a network. Traffic and routes characterize the dynamic nature of the homeostatic system; however, signal flow has not been identified.

The analysis of signal flow requires simultaneous, global, multiple "omic" measurements under the same conditions. Quantitative and global measurements in a single omic layer by use of omic technology are now available (Bertone et al., 2004; Fiehn et al., 2000; Fischer and Sauer, 2005; Ghaemmaghami et al., 2003; Ishihama et al., 2005; Iwasaki et al., 2010; Nilsson et al., 2010; Olsen et al., 2006; Soga et al., 2002). Measurements in a single omic layer are often used in the screening of molecules for specific cellular functions rather than in the identification of trans-omic networks (Bartke et al., 2010; Lowery et al., 2007; O'Connell et al., 2010). Connecting measurements of different omic layers under different experimental conditions could allow for the identification of possible trans-omic networks. However, because molecular interactions between multiple omic layers are mutually connected, signals that flow in a trans-omic network cannot be reconstructed by integrating individual measurements in single omic layers under different conditions; instead, these signals should be reconstructed using simultaneous quantitative measurements across trans-omic layers under the same conditions (Wiley, 2011). A reconstruction method for the signal flow in a trans-omic network based on simultaneously measured trans-omic data has not yet been established.

Hormones regulate cellular homeostasis through selective temporal control of multiple signaling pathways to exert specific functions. Many hormones show distinct temporal patterns in vivo (Brabant et al., 1992). For example, blood insulin, which
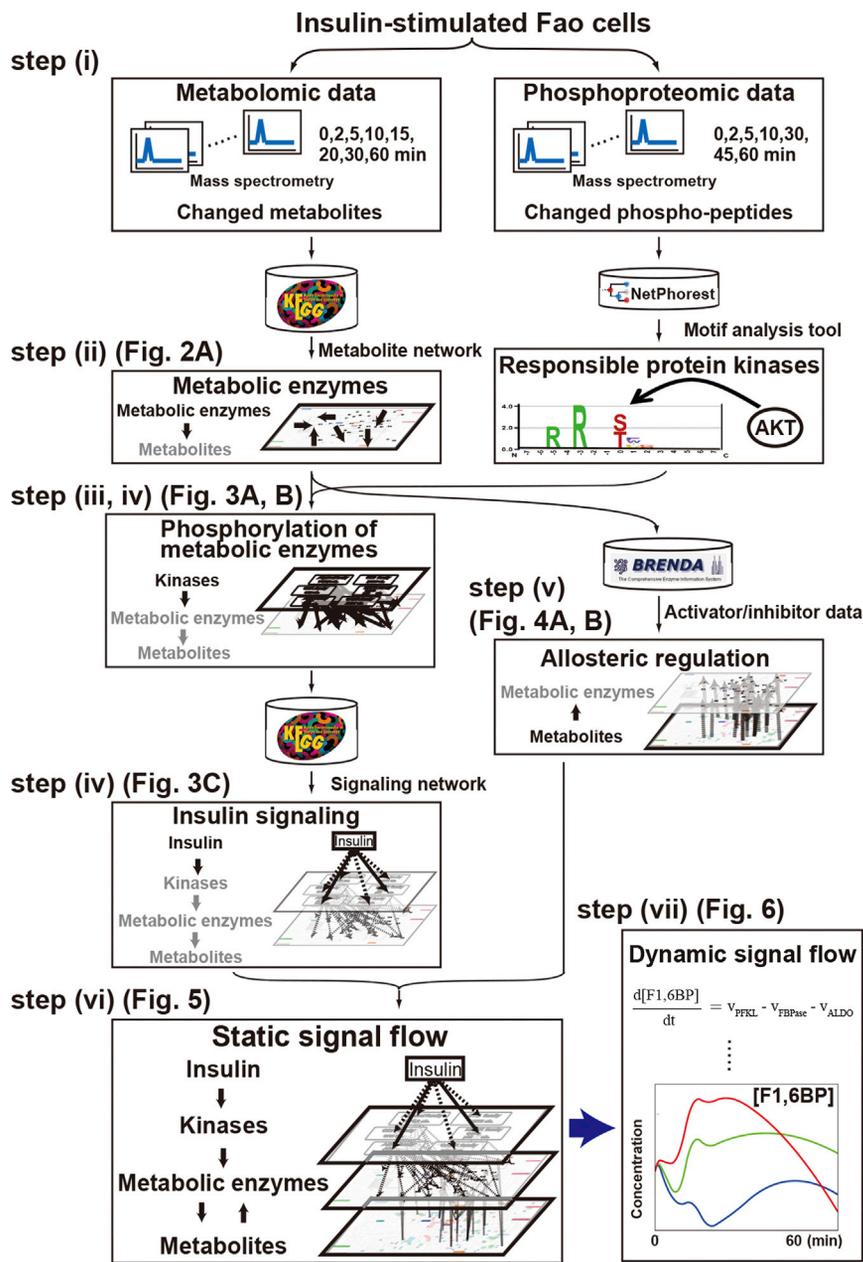
Insulin-stimulated Fao cells

Figure 1. Procedures of Reconstruction of Signal Flow in the Trans-Omic Network
The procedures for the reconstruction of the signal flow are based on phosphoproteome and metabolome data, which consist of seven successive steps of retracing metabolites (the final output of the system) to insulin (the input to the system). The detailed procedures can be found in Supplemental Experimental Procedures. See also Figure S2 and Table S1.

In this study, we analyzed the signal flow of acute insulin action in rat hepatoma FAO cells, which showed insulin-dependent signaling activities similar to those of primary hepatocytes (Kubota et al., 2012). We developed the reconstruction method of a static signal flow in a trans-omic network using multiple omic data and databases and identified the static signal flow of acute insulin action by retracing from the outputs of the system (metabolites) to the input (insulin). We analyzed the dynamic signal flow of insulin-dependent glycolysis using experiments with phospho-mimetic mutants of liver-type phosphofructokinase 1 (PFKL), a key enzyme of glycolysis in the liver, and kinetic modeling. We found that insulin induces phosphorylation and activation of PFKL and controls a key reaction in glycolysis.

RESULTS

Procedures for Reconstruction of Signal Flow in a Trans-Omic Network

We attempted to identify signal flow in a trans-omic network of acute insulin action based on trans-omic data (Figure 1; Experimental Procedures). We measured time-course data from the metabolome, phosphoproteome, and transcriptome of acute insulin action (<60 min) under the same conditions in FAO cells (Figure S1A), which consisted of 304 metabolites, 7,277 phosphorylated sites on 3,458 proteins, and 19,778 RNA probes (Table S1; Figure S1B). Messenger RNAs of only two related metabolic enzymes, including glucose-6-phosphatase (G6Pase), changed within 60 min. G6Pase is known as a key enzyme of gluconeogenesis and is rapidly responsive to insulin (Figure S2A). However, the abundance of protein in G6Pase did not vary within 60 min (Figure S2B). Therefore, we excluded the contributions of protein and mRNA expression in acute insulin action in this study. We postulated that acute insulin action in metabolic control is primarily regulated by enzymatic activities via protein phosphorylation and allosteric regulation rather than

is a key hormone for metabolic homeostasis (Whiteman et al., 2002), reportedly exhibits several specific temporal patterns, including additional secretion that is transiently observed in response to meals and basal secretion that is characterized by persistently low circulating insulin concentrations (Lindsay et al., 2003; Polonsky et al., 1988). We have previously shown that insulin selectively changes the signal flow through signaling pathways, depending on the temporal patterns (Kubota et al., 2012; Noguchi et al., 2013). However, signal flow in a limited local network was analyzed in previous studies (Kubota et al., 2012; Noguchi et al., 2013), and the static signal flow and dynamic signal flow of insulin in a whole trans-omic network have yet to be uncovered.

by gene and protein expression. We analyze chronic insulin action (>60 min) involving gene and protein expression in a separate study.

We developed a reconstruction method of signal flow in a trans-omic network of protein phosphorylation and allosteric-regulation-dependent metabolism by acute insulin action. The reconstruction method consists of the following seven procedural steps (Figure 1; Experimental Procedures): (i) identification of quantitatively changed metabolites (outputs of the system); (ii) identification of "responsible metabolic enzymes" that potentially regulate metabolite levels; (iii) identification of protein phosphorylation of responsible metabolic enzymes; (iv) identification of protein-kinase-dependent insulin signaling; (v) identification of the allosteric regulation; (vi) reconstruction of static signal flow in a whole trans-omic network by integrating the results from steps i through v; and (vii) kinetic modeling of dynamic signal flow in the glycolytic pathway, which is one of the local trans-omic networks.

Reconstruction of Static Signal Flow in a Trans-Omic Network

Step i: Identification of Quantitatively Changed Metabolites

We identified quantitatively changed metabolites and their responsible metabolic enzymes and mapped them to the global map provided in the Kyoto Encyclopedia of Genes and Genomes (KEGG) PATHWAY database (Kanehisa et al., 2012), which includes a comprehensive metabolic pathway topology (Figures 2 and S3; Table S1). Hereafter, we refer to this map as the KEGG global metabolism map. We succeeded in measuring 304 metabolites and observed that 44 metabolites were significantly changed (27 increased and 17 decreased) in response to insulin stimulation (Figures 2 and S1B; Table S1). Not all of the measured metabolites and enzymes are shown in Figure 2A because the KEGG global metabolism map does not include all of the known metabolites. Eleven metabolites were mapped on glycolysis, ten metabolites were mapped on the TCA cycle, and 81 were mapped on proteogenic amino acid metabolism (Figure 2; Table S1). In central carbon metabolism, there was a decrease in the upstream metabolites of glycolysis, including glucose 6-phosphate (G6P; Figure 2A, no. 8) and fructose 6-phosphate (F6P; Figure 2A, no. 6). In contrast, there was an increase in the downstream metabolites of glycolysis such as fructose 1,6-bisphosphate (F1,6BP; Figure 2A, no. 14), 3-phospho-D-glycerate (3PG; Figure 2A, no. 12), 2-phospho-D-glycerate (2PG; Figure 2A, no. 16), and phosphoenolpyruvate (PEP; Figure 2A, no. 4). In the TCA cycle, five metabolites were increased including citrate (Figure 2A, no. 11), 2-oxoglutarate (Figure 2A, no. 2), succinyl-CoA (Figure 2A, no. 7), fumarate (Figure 2A, no. 9), and malate (Figure 2A, no. 17). In the glycogen metabolism pathway, glycogen increased (Figure 2A, no. 22). These observations imply that there is an insulin-dependent, large-scale migration of carbons from glycolysis to the TCA cycle and glycogenesis in central carbon metabolism.

Several metabolites in adjacent locations in the metabolic pathways showed positive correlations with each other over time (Figure 2B). These metabolites are likely to compose a "rapid-equilibrium metabolite pool" in which the metabolites are in rapid equilibrium and exhibit similar time courses (Camacho et al., 2005; Palsson, 2011). We defined a group of metabolite pairs that resided within two enzyme steps from one another in the metabolic pathway and that had time courses with a correlation of $r \geq 0.8$ (r is the Pearson correlation coefficient) and composed a rapid-equilibrium metabolite pool. If a pair of metabolites two enzyme steps away is connected only via hub metabolites such as ATP, then the pair was excluded from the pool to filter out trivial metabolite pairs. The hub metabolites were determined according to previous studies of network topology (Table S2) (Alves et al., 2002). We found six rapid-equilibrium metabolite pools: three pools in glycolysis (Figure 2, P1, P2, and P3); one large pool including the TCA cycle (Figure 2, P6); one pool in nucleotide metabolism (Figure 2, P4); and one pool involving acetylglucosamine phosphates (Figure 2, P5; Table S2). The two glycolytic pools (P1 and P3) (Bennett et al., 2009; Camacho et al., 2005; Palsson, 2011; Wittmann et al., 2005) and part of the pool around the TCA cycle (P6) (Wittmann et al., 2005) previously have been reported as rapid-equilibrium metabolite pools indicating that our analysis successfully identified the known metabolic changes. The other pools (Figure 2, P2, P4, and P5; Table S2) are novel. The correlation coefficients between the metabolite pairs in the rapid-equilibrium metabolic pools were statistically significant (p < 0.001). Most of the metabolite pairs not in the rapid-equilibrium metabolic pools did not exhibit statistical significance (p > 0.1) (Table S2).

Step ii: Identification of Responsible Metabolic Enzymes

Changes in the levels of a metabolite are caused by changes in the reaction rates of the production (influx) or consumption (efflux) of that metabolite. A reaction rate is determined by the enzymatic activity, amount of enzyme, amount of substrate, and product levels. Hereafter, we define the enzymes that directly produce or consume at least one quantitatively changed metabolite as "responsible metabolic enzymes." In other words, a changed metabolite is a substrate or a product of responsible metabolic enzymes. We identified 198 responsible metabolic enzymes for 44 changed metabolites from the KEGG PATHWAY database (Figure 2A, black lines; Figure S1B). Only 25 of the 44 changed metabolites and 132 of the 198 responsible metabolic enzymes are exhibited in Figure 2A. Hereafter, the number of enzymes is counted in terms of enzyme commission (EC) numbers (IUBMB, 1999). Changes in the activities of responsible metabolic enzymes can be regulated by phosphorylation and allosteric regulation via metabolites.

Step iii: Identification of Protein Phosphorylation of Responsible Metabolic Enzymes

We examined protein phosphorylation of responsible metabolic enzymes, which can potentially change their enzymatic activities (Figure 3A). From the phosphoproteomic data, 199 phosphopeptides derived from 49 responsible metabolic enzymes were identified (Figure S1B). Among these phosphopeptides of the responsible metabolic enzymes, we selected quantitatively changed phosphopeptides. A total of 106 phosphopeptides of 26 responsible metabolic enzymes were selected as the significantly phosphorylated phosphopeptides (Figures 3A and S1B; Table S3). These 26 phosphorylated responsible metabolic enzymes corresponded with 19 quantitatively changed metabolites (Figure 3A). We found that 23 phosphorylated sites of the

A

Responsible metabolic enzymes ●━━●

B
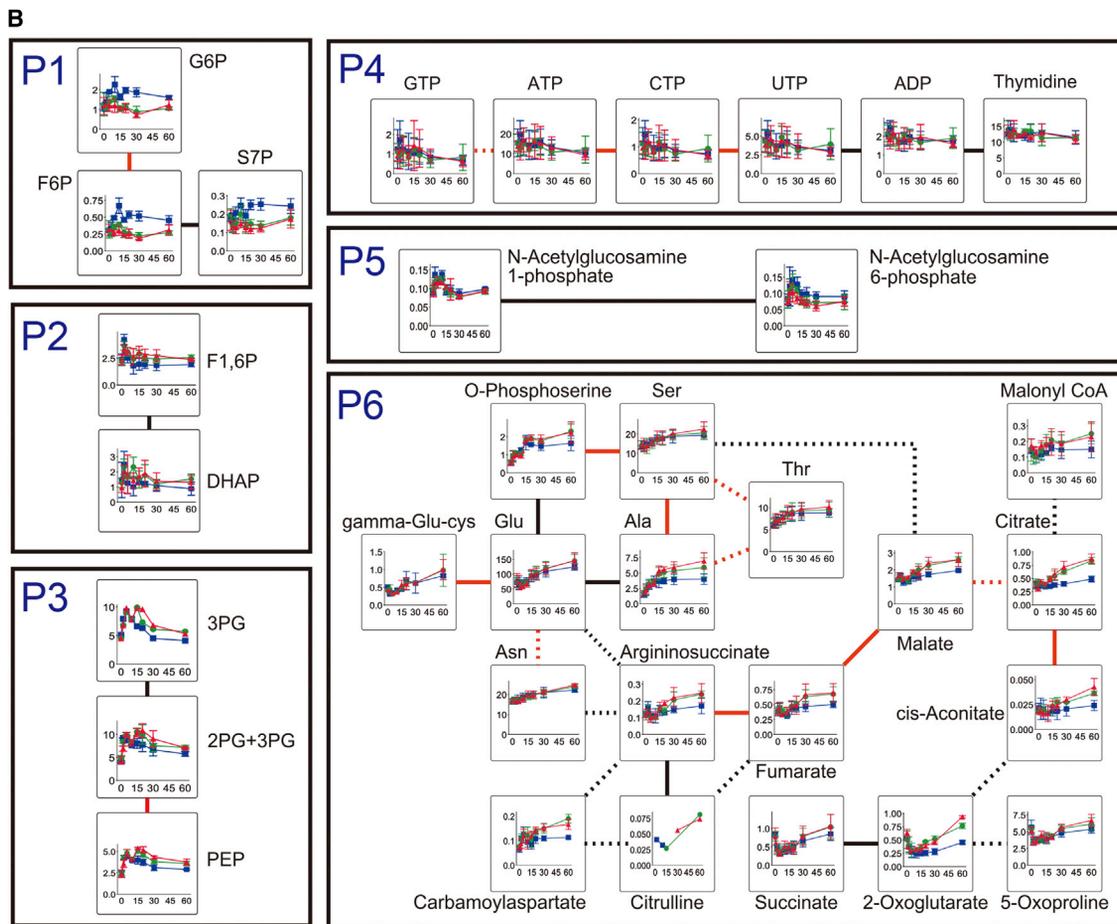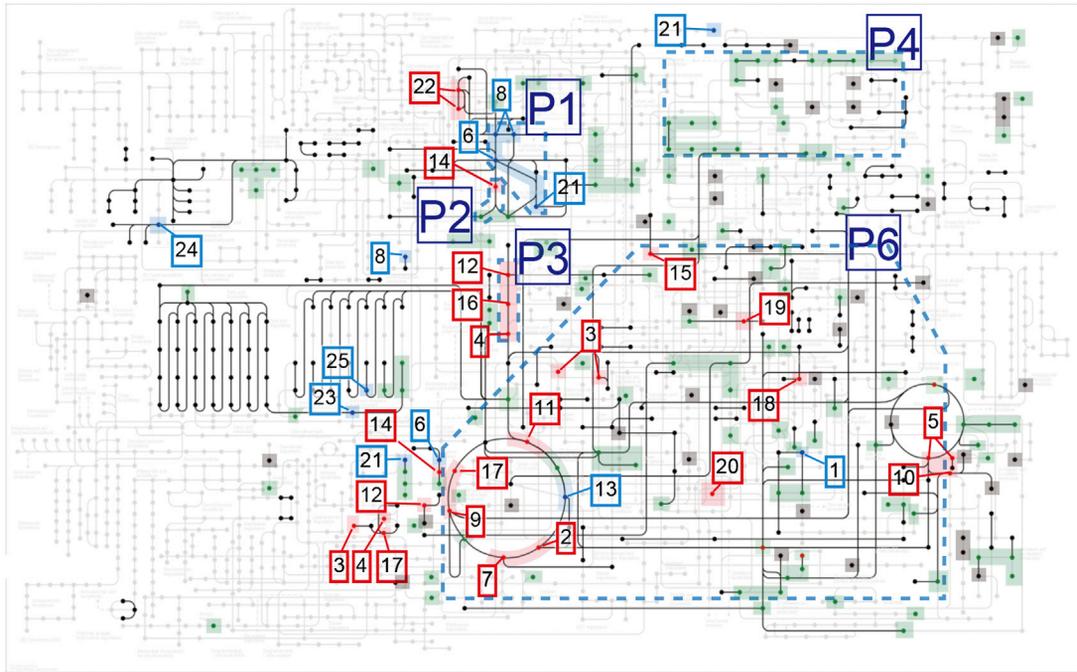
(legend on next page)

responsible metabolic enzymes had already been registered in the PhosphoSitePlus (http://www.phosphosite.org) database (Hornbeck et al., 2012) and that 48 phosphorylated sites of the responsible metabolic enzymes were novel. One phosphorylation site could be covered by multiple phosphopeptides. Some responsible metabolic enzymes with insulin-dependent phosphorylation, including ATP-citrate lyase (ACLY) at S455 (Berwick et al., 2002), carbamoyl-phosphate synthetase 2 (CAD) at S1859 (Hsu et al., 2011), and 6-phosphofructo-2-kinase/fructose 2,6-bisphosphatase (PFKFB3) at S461 (Atsumi et al., 2005) have already been reported, indicating that our analysis successfully identified the known protein phosphorylation of the responsible metabolic enzymes. Given that phosphorylation of responsible metabolic enzymes is considered to be relayed by the protein phosphorylation-dependent signaling network of insulin, these 26 phosphorylated responsible metabolic enzymes are potential primary targets of insulin signal flow in the metabolome layer.

Step iv: Identification of Protein-Kinase-Dependent Insulin Signaling

Next, we attempted to identify the signal flow in the protein-kinase-dependent insulin-signaling network that connects insulin to the responsible metabolic enzymes. First, we identified potential upstream protein kinases for the phosphorylated responsible metabolic enzymes through the amino acid sequences of the phosphorylated peptides derived from the responsible metabolic enzymes (Table S3). Hereafter, we denote these upstream kinases as "responsible protein kinases" for responsible metabolic enzymes. We selected the most probable kinases predicted by NetPhorest as the responsible protein kinases (see Table S3 for distributions of scores [posterior probability] for each phosphorylation site). NetPhorest is an analytical tool that predicts responsible protein kinases by probabilistic models using the amino acid sequence of phosphopeptide (Miller et al., 2008). We identified 13 responsible protein kinases of the phosphorylated responsible metabolic enzymes as a whole (Figures 3B and S1B; Table S3). Hereafter, we counted the numbers of the responsible protein kinases using the kinase classifiers of NetPhorest. These 13 responsible protein kinases include AKT, glycogen synthase kinase-3β (GSK3β), and p70 ribosomal protein S6 kinase (p70S6K), which are key signaling molecules in the insulin-signaling pathway. With the phosphorylated responsible metabolic enzymes in step iii, we connected the insulin-signaling pathway map provided by the KEGG PATHWAY database to the responsible protein kinases (Figure 3C). Hereafter, we refer to the insulin-signaling pathway map in Figure 3C as the insulin-signaling pathway. Among the 13 responsible protein kinases, five kinases (AKT, GSK3β, p70S6K, PKA, and PKC; Figure 3C) were connected to the insulin-signaling pathway and eight kinases (AKT, CK2, CLK, GSK3, NEK1, PKA, PKC, and p70S6K; Table S3) were phosphorylated (Figure S1B). There were 71 phosphorylation sites on the 26 responsible metabolic enzymes connected to the 13 responsible protein kinases (Table S3; Figure S1B). The resulting insulin-signaling pathway included the phosphorylation of signaling molecules, such as IRS, Raptor, TSC1, and S6 (Cheng et al., 2010), the responsible protein kinases, such as AKT, GSK3β, p70S6K, and ERK1/2 (Cheng et al., 2010), and the phosphorylated responsible metabolic enzymes, such as ACLY (Berwick et al., 2002) and liver-type phosphofructokinase 1 (PFKL), which catalyze F6P into F1,6BP, a key enzyme in glycolysis (Figure 3C). This result indicates that our analysis successfully identified the known protein phosphorylation of the responsible metabolic enzymes and demonstrates how insulin transmits its signal to the responsible protein kinases and responsible metabolic enzymes through the signaling pathways.

Step v: Identification of Allosteric Regulation

In addition to the protein phosphorylation-dependent changes in the activities of the responsible metabolic enzymes, the activities of the responsible metabolic enzymes are regulated by allosteric effectors (activators and inhibitors) that are metabolites (Figure 4A). We searched the allosteric effectors of all the responsible metabolic enzymes (198 enzymes) from the BRENDA (http://www.brenda-enzymes.org/) database (see Experimental Procedures) (Schomburg et al., 2013), which provides information regarding allosteric effectors and their target enzymes from a comprehensive literature search. We found that 35 quantitatively changed metabolites function as allosteric effectors for the 94 responsible metabolic enzymes via 226 allosteric regulation (36 activation, 190 inhibition) (Figure 4B; Figure S1B; Table S4). A metabolite can operate as an activator for some enzymes and as an inhibitor for others. We also found quantitative changes in 24 substrates for 74 responsible metabolic enzymes and 25 products for 122 responsible metabolic enzymes from the KEGG PATHWAY database (Figures 4C and 4D; Table S4).

Step vi: Reconstruction of the Static Signal Flow of Acute Insulin Action in a Trans-Omic Network

We integrated the results of steps i through v and reconstructed the static signal flow of acute insulin action in a trans-omic network (Figure 5; Movie S1). An insulin signal was first transmitted through insulin receptors (IRs) to signaling pathways including the 13 responsible protein kinases, such as AKT and


Figure 2. Identification of Quantitatively Changed Metabolites and Responsible Metabolic Enzymes Corresponding to Steps i and ii

(A) Quantitatively changed metabolites and responsible metabolic enzymes projected on the KEGG global metabolism map. Dots represent metabolites and black lines represent responsible metabolic enzymes. For the metabolites, the dots with red, blue, and green backgrounds represent an increase, decrease, and no changes in response to insulin, respectively. Numbers adjacent to the dots are unique identifiers of quantitatively changed metabolite, which are presented together with corresponding metabolite names in Table S1. The numbers surrounded by red and blue indicate the metabolite was increased or decreased, respectively, in response to insulin stimuli. P1 through P6 indicate the locations of six rapid-equilibrium metabolite pools (surrounded by dashed lines) (Supplemental Experimental Procedures).

(B) The time courses of metabolites in rapid-equilibrium metabolic pools (P1–P6). The means and SDs of three independent points are shown. The unit for the metabolite concentration is 1 nmol/1.7×10^7 cell. Insulin concentrations are as follows: 0.01 nM (blue); 1 nM (green); and 100 nM (red). The bold and dashed lines between the metabolites represent that the metabolites are one enzyme step away and two enzyme steps away, respectively. The colors of the lines between the metabolites correspond to Pearson correlation coefficients (red: $r \geq 0.9$; black: $0.8 \leq r < 0.9$).

See also Figure S3 and Table S2.

A   Phosphorylated responsible metabolic enzymes

B

C
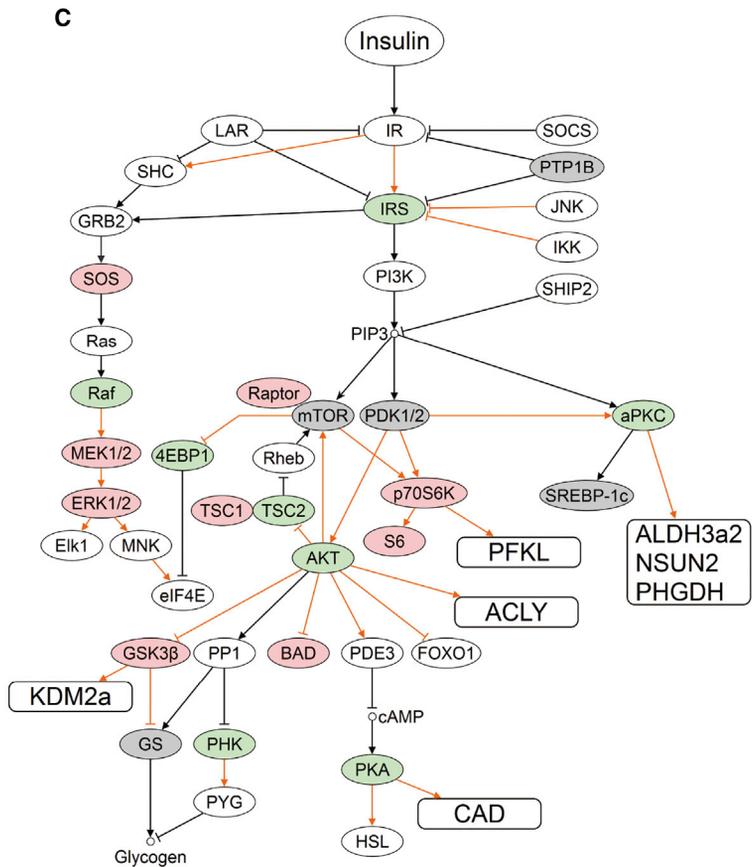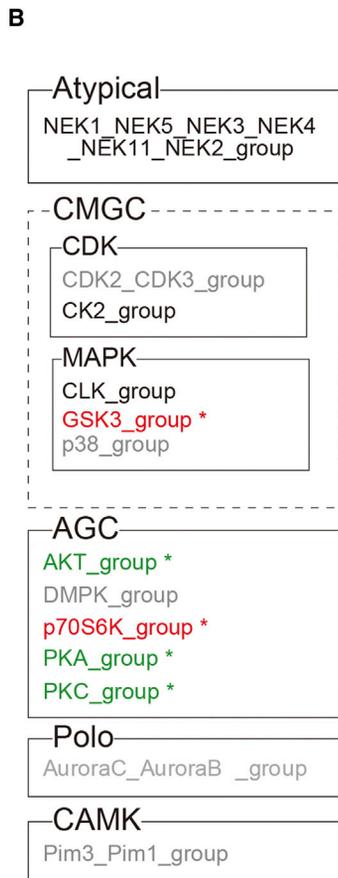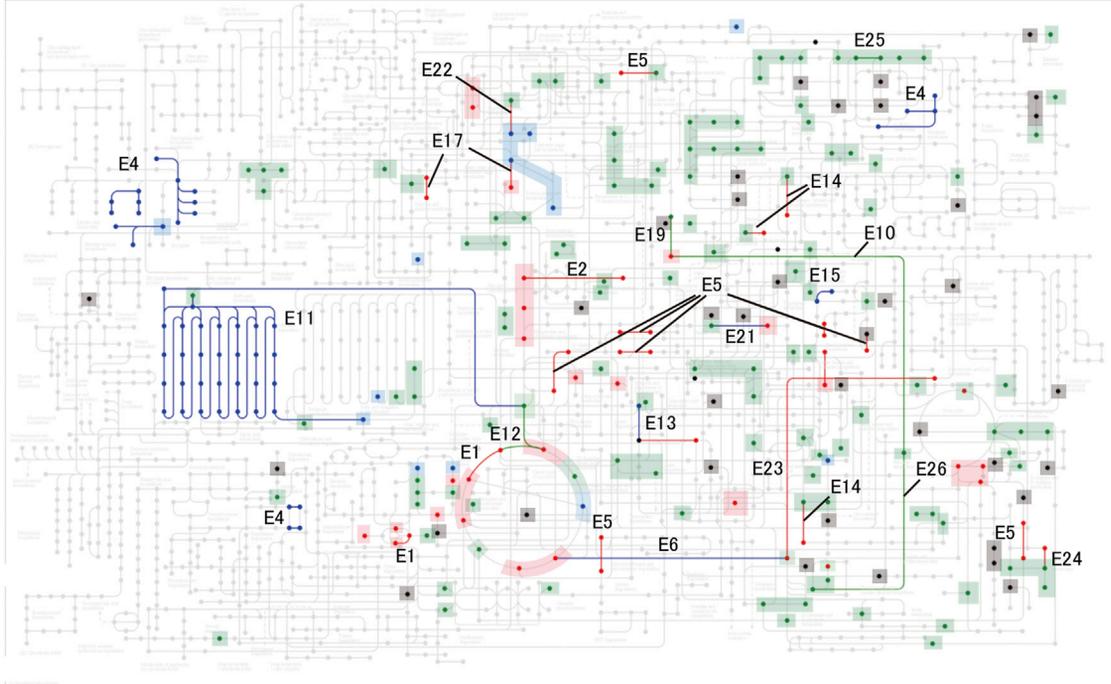
(legend on next page)

p70S6K (Figure 5, top layer; Figure S1B). The responsible protein kinases potentially transmit a signal to the 26 phosphorylated responsible metabolic enzymes through 71 phosphorylation sites (Figure 5, orange arrows from the top to the middle layer; Figure S1B). A protein kinase can phosphorylate multiple metabolic enzymes, and a metabolic enzyme can be phosphorylated by multiple kinases. The 35 changed metabolites serve as allosteric effectors and feedback signals to the 94 responsible metabolic enzymes through 36 activation and 190 inhibition (Figure 5, red and blue arrows from the bottom to the middle layer; Figure S1B). The 198 responsible metabolic enzymes, including 26 phosphorylated and 94 allosterically regulated enzymes, led to changes in the 44 metabolites (Figure 5, white arrows from the middle to the bottom layer; Figure S1B). The integration of steps i through v revealed the global landscape of the signal flow of acute insulin action in a trans-omic network (Figure 5).

Reconstruction of Dynamic Signal Flow in a Trans-Omic Network of Glycolytic Pathway
Step vii: Reconstruction of Dynamic Signal Flow in a Glycolytic Pathway of a Local Trans-Omic Network
We next examined the dynamic signal flow of insulin and attempted to construct a kinetic model of the trans-omic networks based on the time-course omic data. However, because there were many unmeasured metabolites, we could not develop the kinetic model of the whole trans-omic network. Instead, we focused on a local trans-omic network of the glycolytic pathway between F6P and F1,6BP because of three reasons: insulin induced phosphorylation of PFKL, a key enzyme in glycolysis; F6P together with upstream molecules decreased (Figure 2B, P1), whereas F1,6BP together with downstream molecules increased (Figure 2B, P2 and P3), and F6P and F1,6BP exhibited a strong negative correlation ($r = -0.552$), indicating that insulin facilitates conversion of F6P into F1,6BP, and all metabolites surrounding F6P and F1,6BP were measured (Figure 6A), which is necessary for development of a kinetic model. Because the functional role of phosphorylation at S775 of PFKL remains unknown, we first examined the effect of phosphorylation at S775 of PFKL on its kinase activity by making phospho-mimetic (S775D or S775E) and nonphospho-mimetic (S775A) mutants (Figure 6B). Both phospho-mimetic PFKL mutants (S775D or

S775E) exhibited increased kinase activity compared with the wild-type PFKL, whereas the nonphospho-mimetic mutant (S775A) did not (Figure 6B), indicating that insulin phosphorylates and activates PFKL. PFKL activity is regulated positively by fructose-2,6-bisphosphate (F2,6BP); it is regulated negatively by citrate, PEP, isocitrate, 2-oxolgutarate and malate (Passonneau and Lowry, 1963) (Figure 6A). PFKL activity also has been shown to be regulated by ATP, ADP, AMP, and other metabolites (Mor et al., 2011; Schöneberg et al., 2013); however, because these metabolites were unchanged in response to insulin (Table S1), they were not considered in this study. The reverse reaction, conversion of F1,6BP to F6P, is catalyzed by a different enzyme, fructose-1,6-bisphosphatase (FBPase), whose activity is regulated negatively by F2,6BP (Rakus et al., 2000) and positively by citrate (Nimmo and Tipton, 1975) (Figure 6A).

We examined which phosphorylation and allosteric regulation selectively contributed to conversion between F6P and F1,6BP using a kinetic model of dynamic signal flow of insulin in the glycolytic pathway (Figure 6C; Supplemental Experimental Procedures). In our experiments, there was a transient and sustained increase of F1,6BP (Figure 6C, dots); however, in our simulations, only sustained increase of F1,6BP was reproduced (Figure 6C, lines). This suggests the existence of the unknown signal flow responsible for the transient increase of F1,6BP. We examined which phosphorylation and allosteric regulation selectively contributed to sustained increase of F1,6BP by variable selection in the kinetic model (Figure 6D; Supplemental Experimental Procedures). We selected five variables as the minimum set governing the dynamic signal flow (Figures 6D and S4A). The five variables included phosphorylation of PFKL at S775 and allosteric regulation by F2,6BP, PEP, citrate, and malate (Figures 6D and 6E). We made a kinetic model with five variables. This model appeared to be comparable with the original full model using eight variables (Figures 6E and S4B), confirming that the five variables we used are the dominant factors for dynamic signal flow between F6P and F1,6BP (Figure 6E). Given that PEP, citrate, and malate are downstream of F1,6BP, these metabolites serves as negative-feedback regulators for F1,6BP production (Figures 6E, dashed line; Figures S4C–S4E), consistent with previous observations (Nimmo and Tipton, 1975; Passonneau and Lowry, 1963; Rakus et al., 2000). Insulin positively regulates F1,6BP

Figure 3. Identification of Protein-Kinase-Dependent Insulin Signaling to Responsible Metabolic Enzymes Corresponding to Steps iii and iv
(A) Identification of protein phosphorylation of responsible metabolic enzymes (step iii). Colored lines are phosphorylated responsible metabolic enzymes. Red indicates all of the significantly changed phosphorylation sites of the enzyme exhibited an increase (>1.5-fold) in response to the insulin stimulus. Blue indicates all of the significantly changed phosphorylation sites of the enzyme exhibited a decrease (<0.67-fold) in response to the insulin stimulus. Green indicates all the significantly changed phosphorylation sites of the enzyme exhibited either an increase or a decrease in response to the insulin stimulus. Numbers next to the colored lines (e.g., E3) are unique identifiers for 26 phosphorylated responsible metabolic enzymes, which are presented in Table S3.
(B) The 13 identified responsible protein kinases of phosphorylated metabolic enzymes. Boxes represent superfamilies of each protein kinase based on the kinase tree (Miller et al., 2008). The detailed relationship between the responsible protein kinases and phosphorylated metabolic enzymes can be found in Table S3. The colors indicate the phosphorylated protein kinases; red and green indicate the same information as described in (A). Black indicates the phosphorylation was not changed by insulin. Gray indicates not phosphorylated. *The kinases were included in the insulin-signaling pathway. A dashed box labeled CMGC indicates that CDK and MAPK families belong to the CMGC superfamily.
(C) Identification of protein-kinase-dependent insulin signaling to responsible metabolic enzymes (step iv). An oval corresponds to a protein. The colors of the ovals represent the following phosphorylation states: red and green indicate the same information described in (A) and (B); gray indicates phosphorylation was unchanged by the insulin; and white indicates no phosphorylation. Five kinases out of the 13 responsible kinases were connected to the insulin-signaling pathway (AKT, GSK3β, p70S6K, PKA, and PKC). The names in the boxes are phosphorylated metabolic enzymes. An arrow and a bar-headed arrow indicate activation and inhibition, respectively. Orange denotes phosphorylation and black denotes other molecular interactions.
See Table S3 for the abbreviations of the phosphorylated metabolic enzymes.
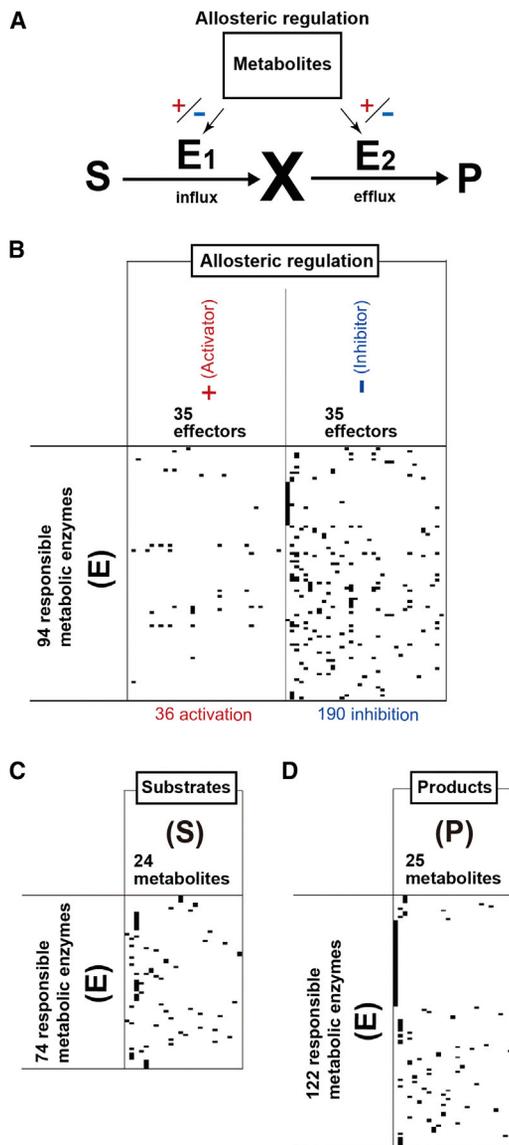
Figure 4. Identification of Allosteric Regulation of Responsible Metabolic Enzymes by Metabolites Corresponding to Step v

(A) The level of a metabolite (X) is determined by the balance between the influxes and effluxes, i.e., the reaction rates of enzymes E_1 and E_2, respectively. S denotes the substrate of E_1, and P is the product of E_2. Here, allosteric regulation includes the regulation of influxes and effluxes by the binding of metabolites acting as allosteric effectors (activators and inhibitors) to the enzymes and by the levels of the substrates and products.

(B) The allosteric regulation of the responsible metabolic enzymes (E) by the allosteric effectors. The row labels are the responsible metabolic enzymes (E), and the column labels are the activators and inhibitors of the influxes and effluxes (Table S4). A black dot is provided at row i column j if a responsible metabolic enzyme of row i is regulated by an allosteric effector of column j. Such information for allosteric regulation was obtained using the BRENDA database (Experimental Procedures).

(C and D) The substrates (S) and the products (P) of the responsible metabolic enzymes (E), respectively. A black dot is provided at row i column j if a metabolite of column j is a substrate or a product of a responsible metabolic enzyme of row i.

See Table S4 for complete information for (B)–(D).

production by phosphorylation of PFKL at S775 and by increasing F2,6BP (Figures S4F and S4G); the latter is a well-known and conserved mechanism throughout eukaryotes (Rider et al., 2004). Our data indicate an additional role for insulin: phosphorylation-dependent regulation of glycolytic enzymes including PFKL. Thus, these results demonstrate that insulin coordinately regulates the dynamic flow in the glycolytic pathway by insulin-dependent activation of PFKL via phosphorylation and increase of F2,6BP and by the negative-feedback loop via downstream allosteric regulators.

DISCUSSION

In this study, we reconstructed static signal flow of acute insulin action in a whole trans-omic network using time-course transomic data combined with multiple databases and analyzed the dynamic signal flow of a local network of the glycolytic pathway using kinetic modeling. We first identified the quantitatively changed metabolites, which are the outputs of the system (step i; Figure 2). We connected the quantitatively changed metabolites and potential responsible metabolic enzymes by using the KEGG global metabolism map (step ii; Figure 2). Among the potential responsible metabolic enzymes, we identified the phosphorylated responsible metabolic enzymes with phosphoproteomic data (step iii; Figure 3A). We connected the phosphorylated responsible metabolic enzymes and the responsible protein kinases with the amino acid sequences of phosphopeptides using the NetPhorest and further connected the responsible protein kinases and insulin-signaling pathway (step iv; Figures 3B and 3C; Table S3). Finally, we connected the allosteric regulation of metabolites to the responsible metabolic enzymes using the BRENDA database (step v; Figures 4A and 4B). Thus, we reconstructed the static signal flow of acute insulin action by retracing the signal flow from the outputs of the system (metabolites) to the input (insulin) (step vi; Figure 5). Moreover, we reconstructed the dynamic signal flow in a local network of the glycolytic pathway using the kinetic modeling with variable selection (step vii; Figure 6).

The reconstruction of dynamic signal flow allowed us to identify a regulation of insulin-dependent glycolysis. We experimentally found that insulin increases phosphorylation at S775 of PFKL, leading to an increase in its kinase activity. With the variable selection of the kinetic model, we demonstrated that insulin can coordinately regulate the dynamic flow between F6P and F1,6BP by insulin-dependent activation of PFKL via phosphorylation and increase of F2,6BP, and by the negative-feedback loop via downstream allosteric regulators. The regulation of the glycolytic pathway by F2,6BP and regulation by the negative-feedback loop via downstream metabolites are well-known and conserved mechanisms throughout eukaryotes (Bloxham and Lardy, 1973; Rider et al., 2004). Moreover, the phosphorylation site of S775 is specific to PFKL (liver-type PFK), but not to other isoforms of PFKs, such as PFKM (muscle-type PFK) or PFKP (platelet-type PFK) (Simpson and Fothergill-Gilmore, 1991). Given that the liver is the main target organ of insulin and that it is specialized for controlling systemic glucose homeostasis, and given the ubiquitous controlling mechanisms by F2,6BP and downstream metabolites, special regulation of glycolysis by insulin may be needed for tight control of glucose
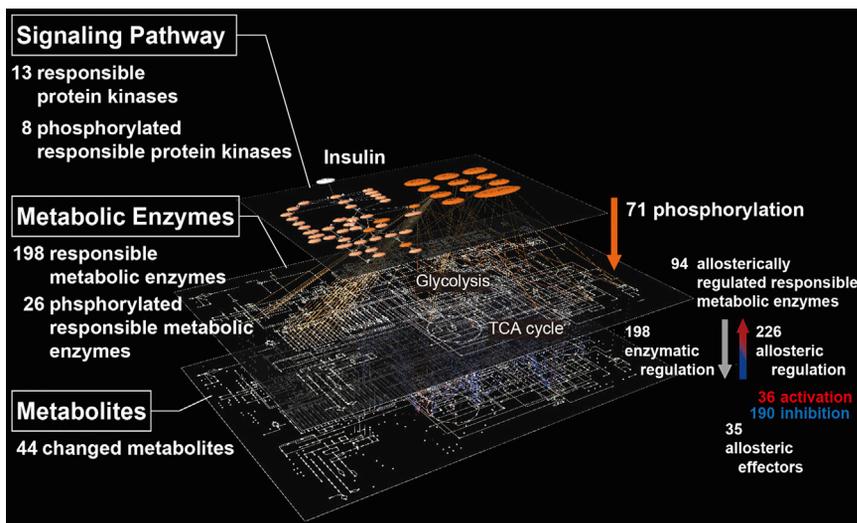
Figure 5. A Global Landscape of the Static Signal Flow of Acute Insulin Action in a Trans-Omic Network by Integrating the Results from Steps i through v Corresponding to Step vi

The insulin signal flows across three layers: the insulin-signaling pathway (the top layer); the metabolic enzymes (the middle layer); and the metabolites (the bottom layer). Orange arrows (from the top to the middle layer) indicate the signal flow from the responsible protein kinases to the responsible metabolic enzymes, white arrows (from the middle to the bottom layer) indicate the signal flow from the responsible metabolic enzymes to the metabolites, and the red and blue arrows (from the bottom to the middle layer) indicate the signal flow of the allosteric regulation (red, activator; blue, inhibitor). A 3D video file and a network structure file of the static signal flow are provided. The 3D video of the static signal flow can be seen in Movie S1.

metabolism in the liver. Our result suggests that insulin-dependent phosphorylation of PFKL at S775 is one such special mechanism of glucose metabolism in the liver. Further study is necessary to address the role of phosphorylation of PFKL at S775 in glucose metabolism in the liver.

The reliability of the signal flow analysis depends on the quality and quantity of the trans-omic data, the criteria for the selection of the data, and the comprehensiveness and reliability of the information available in the databases. With respect to the quality of the trans-omic data, the current metabolome and phosphoproteome data did not fully encompass all of the metabolites and phosphopeptides, mostly because of technical reasons, such as the lack of standard samples for some metabolites and the low sensitivity of detection of the phosphopeptides. Regarding the quantity of the trans-omic data, the sample numbers of the trans-omic data, especially phosphoproteomic data, were limited because of the slow throughput speed.

This method relies on several selection criteria such as the fold change for selecting the changed metabolites and phosphopeptides and a residual sum of squares for selecting essential variables by variable selection. Because other criteria might improve the reliability of our analysis, other criteria should be tested in the future. For comprehensiveness and reliability of the information available in the databases, we used the KEGG PATHWAY database for a global metabolic map and the insulin-signaling pathway, the latter of which does not encompass all of the signaling molecules. We used the NetPhorest to connect the phosphorylated metabolic enzymes to protein kinases. Because many protein kinases recognize a similar consensus motif of amino acid sequences of substrates, some of the relationships between the metabolic enzymes and protein kinases might not be accurately predicted and should be experimentally tested further. Additionally, information regarding biological and cellular contexts such as colocalization and network could be used for predicting in vivo kinase-substrates relationships (Joughin et al., 2012; Linding et al., 2007). We used the BRENDA database for identifying allosteric regulation. In general, the allosteric regulation has been examined in vitro, and it is difficult to validate the

allosteric regulation at the cellular level. Here, we propose kinetic modeling with the variable selection method to eliminate the nonessential variables and to identify the essential variables for dynamic signal flow. In addition, because the numbers and quality of the trans-omic data in this study might not be sufficient, the parameters in the kinetic model might not be reliable. In the future, when more quantitative high-throughput omic technology becomes available, this problem will be solved and our method will become more valid and useful.

Trans-omic analyses of global networks of metabolic control in *Escherichia coli* (Ishii et al., 2007), *Bacillus subtilis* (Buescher et al., 2012), and *Saccharomyces cerevisiae* (Oliveira et al., 2012) have been reported. Ishii et al. measured transcripts, protein abundance, metabolites, and metabolic fluxes of *E. coli* under four growth conditions and 24 disruptants; they found that the metabolite levels remained stable against environmental perturbations by enzyme-level regulation and against genetic perturbation by flux rerouting (Ishii et al., 2007). Buescher et al. measured time courses of transcripts, protein abundance, metabolites, and metabolic fluxes of *B. subtilis* using two nutrient-shift experiments and also identified transcriptional regulatory networks based on chromatin immunoprecipitation (ChIP)-on-chip (Buescher et al., 2012). They analyzed the mechanism of adaptation to malate and glucose across the transcriptome layer and the metabolome/fluxome layer and showed that the metabolic fluxes of *B. subtilis* are primarily changed by transcriptional regulation when the nutrient source is shifted from malate to glucose, but that posttranscriptional modulation is utilized when the nutrient shift is from glucose to malate. Oliveira et al. measured protein phosphorylation and metabolites of *S. cerevisiae* and combined them with protein abundance and flux data (Oliveira et al., 2012). These authors concluded whether the phosphorylation of metabolic enzymes work positively or negatively regarding reaction rates of the enzymes based on the correlations of phosphorylation and flux; this has been further confirmed by measuring the concentration of substrates and products of the enzymes. Furthermore, recent advances allow systematic identification of allosteric protein-metabolite
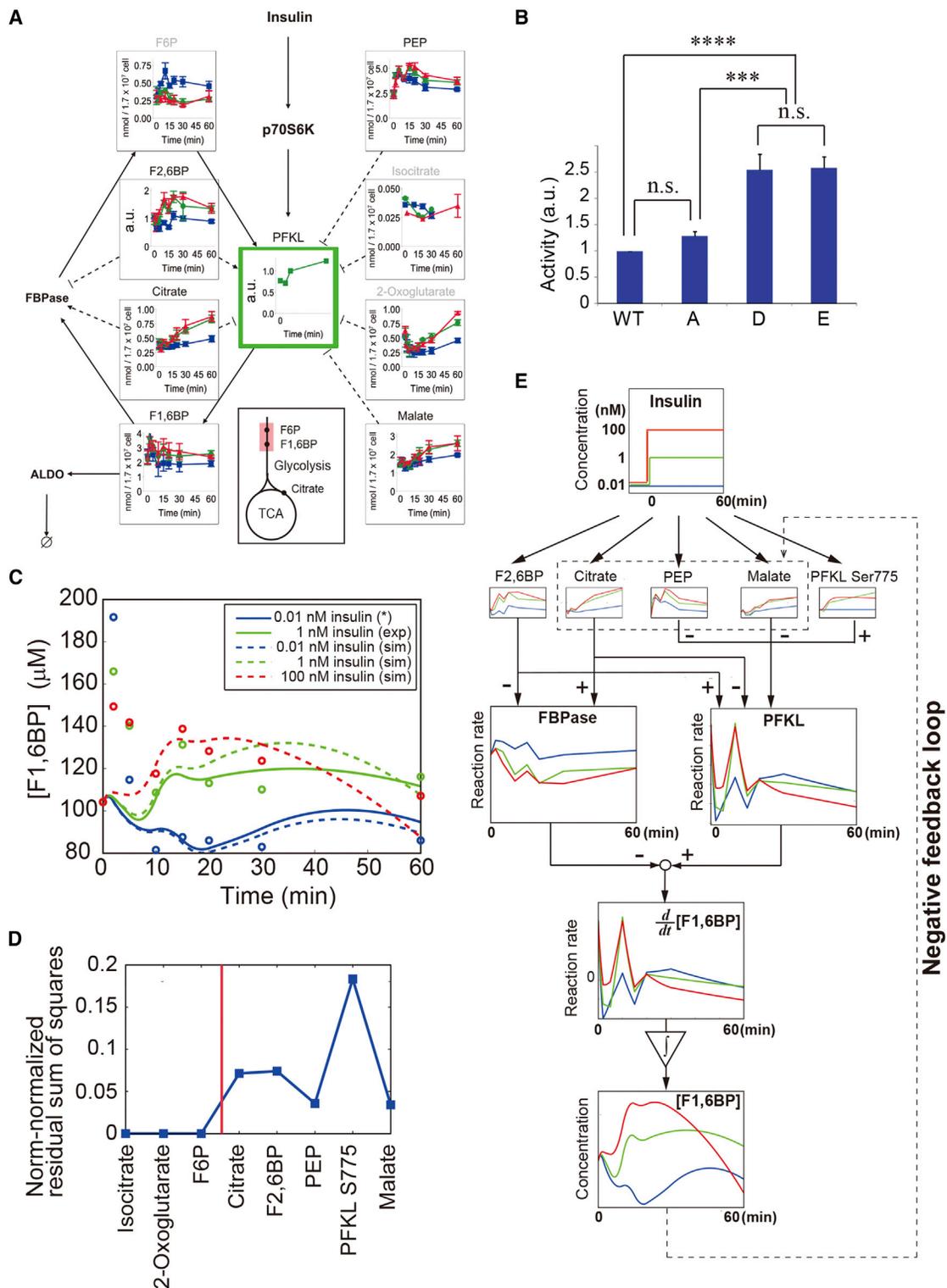
Figure 6. Analysis of the Dynamic Signal Flow in a Local Trans-Omic Network of Conversion of F6P to F1,6BP Corresponding to Step vii

(A) The local trans-omic network of F1,6BP regulation. White boxes and green boxes indicate metabolites and metabolic enzymes, respectively. Solid arrows indicate enzymatic reactions. Dashed lines with arrow heads and with flat heads indicate the allosteric regulation of activators and inhibitors, respectively. Black and gray metabolites are essential and nonessential variables, respectively (see D). The location of the network in central carbon metabolism is indicated by red (inset). ALDO, aldolase. The other abbreviations for the molecules are shown in Table S5.

interactions that control enzyme activity in vivo (Link et al., 2013). In addition to these trans-omics studies, phosphoproteomic analysis is extensively used to estimate interaction networks in insulin signaling (Friedman et al., 2011; Humphrey et al., 2013; Monetti et al., 2011) and other signaling networks (Jørgensen et al., 2009; Olsen et al., 2006). We measured time-course data for protein phosphorylation and metabolites in mammalian cells in response to insulin and reconstructed static signal flow from insulin to metabolites through phosphorylation and allosteric regulation. We analyzed the dynamic signal flow by kinetic modeling with variable selection and found that insulin coordinately regulates the dynamic flow in the glycolytic pathway by insulin-dependent activation of PFKL via phosphorylation and an increase in F2,6BP, and by the negative-feedback loop via downstream allosteric regulators.

Insulin reportedly exhibits several temporal patterns, including additional secretion (observed in response to meals) and basal secretion (characterized by persistently low circulating insulin concentrations) (Lindsay et al., 2003; Polonsky et al., 1988). We have previously shown that insulin selectively changes the signal flow through signaling pathways depending on the temporal patterns (Kubota et al., 2012). Rapid pulse stimulation of insulin, which resembles additional secretion of insulin in vivo, selectively regulates GSK3β and p70S6K, whereas slow ramp stimulation of insulin, which resembles basal secretion of insulin in vivo, selectively regulates GSK3β and *G6Pase*. In another study, we will apply this method using the trans-omic data in response to pulse and ramp stimulations of insulin and will examine the selective signal flow by the specific temporal patterns of insulin in a trans-omic network. We will also expand our analysis of chronic insulin action by measuring the transcriptome, proteome, lipidome, and epigenome, which would reveal the vital nature of cellular homeostasis.

Because acute cellular functions primarily use protein phosphorylation signaling pathways and secondarily use allosteric regulation to adapt to extracellular stimuli, our method can visualize signal flow from extracellular stimuli through protein phosphorylation pathways and an allosteric regulation network. Our method can be widely applied to identify the signal flow of any growth factors and the signaling network at the cellular and in vivo levels. It would be interesting to apply this method to other growth factors, such as epidermal growth factor and fibroblast growth factors, and to compare signal flow between different types of growth factors and receptors. This type of study would reveal growth factor-specific or receptor type-specific regulation from the viewpoint of signal flow in a trans-omic network, which is characterized by different modes of action at the systems level.

EXPERIMENTAL PROCEDURES

The detailed experimental procedures can be found in Supplemental Experimental Procedures.

Cell Treatments and Comprehensive Measurements

Rat hepatoma FAO cells were stimulated by the indicated doses of insulin and were used for phosphoproteome and metabolome measurements. The phosphoproteome data and metabolome data were processed to reconstruct the static and dynamic signal flows of insulin by using the following seven steps.

Reconstruction of Static and Dynamic Signal Flow in a Trans-Omic Network

Step i: S_1 / S_0 values (see Figure S3 and Supplemental Experimental Procedures for definition) of each metabolite were calculated to identify quantitatively changed metabolites that are equivalent to the metabolites satisfying $| S_1 / S_0 | > 1$.

Step ii: responsible metabolic enzymes that produce or consume at least one quantitatively changed metabolite are identified using the KEGG database in combination with the calculated S_1 / S_0 values.

Step iii: significantly phosphorylated responsible metabolic enzymes were identified using the phosphoproteomic data. A phosphopeptide whose phosphorylation intensity was greater than a 1.5-fold increase or less than 0.67-fold decrease at more than one time point was determined as a quantitatively changed phosphorylation.

Step iv: responsible protein kinases of the significantly phosphorylated responsible metabolic enzymes were estimated using NetPhorest. The responsible protein kinase was connected to the insulin-signaling pathway if it was included in this pathway map.

Step v: the information regarding allosteric effectors acting on the responsible metabolic enzymes was extracted from the BRENDA database.

Step vi: the static signal flow of acute insulin action in a trans-omic network was reconstructed by integrating the results of steps i through v.

Step vii: dynamic signal flow around PFKL was identified using a kinetic model.

PFKL Assay

HEK293 cells transfected with the indicated plasmids harboring cDNA of wild-type and mutants of mouse PFKL were used for PFKL assay to determine the function of phosphorylation of PFKL at S775. We performed a variable selection based on the residual sum of squares between the original full model and reduced models.

ACCESSION NUMBERS

The Gene Expression Omnibus accession number for the microarray data in this article is GSE58302. The mathematical models have been deposited in BioModels Database (Li et al., 2010) and assigned the identifiers MODEL1406130000 and MODEL1406130001.

(B) Enzymatic activities of PFKL. WT, wild-type PFKL. A, D, and E indicate the mutants whose Ser 775 residues were substituted by alanine, aspartate, and glutamate, respectively. The means and SDs of three independent points are shown. *Statistically significant changes between groups determined by a Tukey-Kramer test. ****$p < 0.0001$; ***$0.0001 < p < 0.001$; n.s., not significant ($p > 0.1$).

(C) Time course of F1,6BP in the kinetic model. Solid lines indicate the time course of F1,6BP based on the experimental time-course data of phosphorylation of PFKL at S775 with 1 nM insulin (see Supplemental Experimental Procedures for details). Dashed lines indicate the time course of F1,6BP based on the simulated time course of phosphorylation of PFKL at S775 with 0.01, 1, and 100 nM insulin. The dots indicate experimental data of F1,6BP. Red, green, and blue represent the responses to 100, 1, and 0.01 nM insulin, respectively.

(D) The variable selection with 1 nM insulin stimulation. Residual sum of squares (RSS) of the consecutive variable selections are shown (see Supplemental Experimental Procedures for details). Red indicates the threshold for the variable selection (RSS = 0.001). The five variables above the threshold are essential variables. The variable selection with 100 nM insulin stimulation also provides the same five variables (Figure S4A).

(E) The dynamic signal flow in the kinetic model with the five variables. The time course of F1,6BP is an integration of d[F1,6BP] / dt, which is primarily given by the difference between PFKL and FBPase (Figure S4L).

See also Figure S4.

SUPPLEMENTAL INFORMATION

AUTHOR CONTRIBUTIONS

K.Y., H.K., and S.K. conceived the project. H.K. and S.K. designed the experiments. H.K., Y.T., and R.N. performed the experiments. Y.F. and H.M. provided the DNA construct of PFKL. M.M. and K.I.N. performed the phosphoproteome measurements. K. Kashikura, K.E., K.I., and T.S. performed the metabolome and lipidome measurements. K.Y., H.K., K. Kawata, Y.K., S.U., K. Kunida, and Y.T. analyzed the data. K.Y. and H.K. developed the computational model. K.Y., H.K., and S.K. wrote the manuscript.

ACKNOWLEDGMENTS

REFERENCES

Alves, R., Chaleil, R.A., and Sternberg, M.J. (2002). Evolution of enzymes in metabolism: a network perspective. J. Mol. Biol. 320, 751–770.

Atsumi, T., Nishio, T., Niwa, H., Takeuchi, J., Bando, H., Shimizu, C., Yoshioka, N., Bucala, R., and Koike, T. (2005). Expression of inducible 6-phosphofructo-2-kinase/fructose-2,6-bisphosphatase/PFKFB3 isoforms in adipocytes and their potential role in glycolytic regulation. Diabetes 54, 3349–3357.

Bartke, T., Vermeulen, M., Xhemalce, B., Robson, S.C., Mann, M., and Kouzarides, T. (2010). Nucleosome-interacting proteins regulated by DNA and histone methylation. Cell 143, 470–484.

Bennett, B.D., Kimball, E.H., Gao, M., Osterhout, R., Van Dien, S.J., and Rabinowitz, J.D. (2009). Absolute metabolite concentrations and implied enzyme active site occupancy in Escherichia coli. Nat. Chem. Biol. 5, 593–599.

Bertone, P., Stolc, V., Royce, T.E., Rozowsky, J.S., Urban, A.E., Zhu, X., Rinn, J.L., Tongprasit, W., Samanta, M., Weissman, S., et al. (2004). Global identifi-

cation of human transcribed sequences with genome tiling arrays. Science 306, 2242–2246.

Berwick, D.C., Hers, I., Heesom, K.J., Moule, S.K., and Tavare, J.M. (2002). The identification of ATP-citrate lyase as a protein kinase B (Akt) substrate in primary adipocytes. J. Biol. Chem. 277, 33895–33900.

Bloxham, D.P., and Lardy, H.A. (1973). Phosphofructokinase. In The Enzymes, P.B. Boyer, ed. (New York: Academic Press), pp. 239–278.

Brabant, G., Prank, K., and Schofl, C. (1992). Pulsatile patterns in hormone secretion. Trends Endocrinol. Metab. 3, 183–190.

Brazhnik, P., de la Fuente, A., and Mendes, P. (2002). Gene networks: how to put the function in genomics. Trends Biotechnol. 20, 467–472.

Buescher, J.M., Liebermeister, W., Jules, M., Uhr, M., Muntel, J., Botella, E., Hessling, B., Kleijn, R.J., Le Chat, L., Lecointe, F., et al. (2012). Global network reorganization during dynamic adaptations of Bacillus subtilis metabolism. Science 335, 1099–1103.

Camacho, D., de la Fuente, A., and Mendes, P. (2005). The origin of correlations in metabolomics data. Metabolomics 1, 53–63.

Cheng, Z., Tseng, Y., and White, M.F. (2010). Insulin signaling meets mitochondria in metabolism. Trends Endocrinol. Metab. 21, 589–598.

Feist, A.M., Herrgård, M.J., Thiele, I., Reed, J.L., and Palsson, B.O. (2009). Reconstruction of biochemical networks in microorganisms. Nat. Rev. Microbiol. 7, 129–143.

Fiehn, O., Kopka, J., Dörmann, P., Altmann, T., Trethewey, R.N., and Willmitzer, L. (2000). Metabolite profiling for plant functional genomics. Nat. Biotechnol. 18, 1157–1161.

Fischer, E., and Sauer, U. (2005). Large-scale in vivo flux analysis shows rigidity and suboptimal performance of Bacillus subtilis metabolism. Nat. Genet. 37, 636–640.

Friedman, A.A., Tucker, G., Singh, R., Yan, D., Vinayagam, A., Hu, Y., Binari, R., Hong, P., Sun, X., Porto, M., et al. (2011). Proteomic and functional genomic landscape of receptor tyrosine kinase and ras to extracellular signal-regulated kinase signaling. Sci. Signal. 4, rs10.

Gerosa, L., and Sauer, U. (2011). Regulation and control of metabolic fluxes in microbes. Curr. Opin. Biotechnol. 22, 566–575.

Ghaemmaghami, S., Huh, W.K., Bower, K., Howson, R.W., Belle, A., Dephoure, N., O'Shea, E.K., and Weissman, J.S. (2003). Global analysis of protein expression in yeast. Nature 425, 737–741.

Güell, M., van Noort, V., Yus, E., Chen, W.H., Leigh-Bell, J., Michalodimitrakis, K., Yamada, T., Arumugam, M., Doerks, T., Kühner, S., et al. (2009). Transcriptome complexity in a genome-reduced bacterium. Science 326, 1268–1271.

Hornbeck, P.V., Kornhauser, J.M., Tkachev, S., Zhang, B., Skrzypek, E., Murray, B., Latham, V., and Sullivan, M. (2012). PhosphoSitePlus: a comprehensive resource for investigating the structure and function of experimentally determined post-translational modifications in man and mouse. Nucleic Acids Res. 40, D261–D270.

Hsu, P.P., Kang, S.A., Rameseder, J., Zhang, Y., Ottina, K.A., Lim, D., Peterson, T.R., Choi, Y., Gray, N.S., Yaffe, M.B., et al. (2011). The mTOR-regulated phosphoproteome reveals a mechanism of mTORC1-mediated inhibition of growth factor signaling. Science 332, 1317–1322.

Humphrey, S.J., Yang, G., Yang, P., Fazakerley, D.J., Stöckli, J., Yang, J.Y., and James, D.E. (2013). Dynamic adipocyte phosphoproteome reveals that Akt directly regulates mTORC2. Cell Metab. 17, 1009–1020.

Ishihama, Y., Sato, T., Tabata, T., Miyamoto, N., Sagane, K., Nagasu, T., and Oda, Y. (2005). Quantitative mouse brain proteomics using culture-derived isotope tags as internal standards. Nat. Biotechnol. 23, 617–621.

Ishii, N., Nakahigashi, K., Baba, T., Robert, M., Soga, T., Kanai, A., Hirasawa, T., Naba, M., Hirai, K., Hoque, A., et al. (2007). Multiple high-throughput analyses monitor the response of E. coli to perturbations. Science 316, 593–597.

IUBMB (1999). IUPAC-IUBMB Joint Commission on Biochemical Nomenclature (JCBN) and Nomenclature Committee of IUBMB (NC-IUBMB), newsletter 1999. Eur. J. Biochem. 264, 607–609.

Iwasaki, M., Miwa, S., Ikegami, T., Tomita, M., Tanaka, N., and Ishihama, Y. (2010). One-dimensional capillary liquid chromatographic separation coupled with tandem mass spectrometry unveils the Escherichia coli proteome on a microarray scale. Anal. Chem. *82*, 2616–2620.

Jørgensen, C., Sherman, A., Chen, G.I., Pasculescu, A., Poliakov, A., Hsiung, M., Larsen, B., Wilkinson, D.G., Linding, R., and Pawson, T. (2009). Cell-specific information processing in segregating populations of Eph receptor ephrin-expressing cells. Science *326*, 1502–1509.

Joughin, B.A., Liu, C., Lauffenburger, D.A., Hogue, C.W., and Yaffe, M.B. (2012). Protein kinases display minimal interpositional dependence on substrate sequence: potential implications for the evolution of signalling networks. Philos. Trans. R. Soc. Lond. B Biol. Sci. *367*, 2574–2583.

Joyce, A.R., and Palsson, B.O. (2006). The model organism as a system: integrating 'omics' data sets. Nat. Rev. Mol. Cell Biol. *7*, 198–210.

Kanehisa, M., Goto, S., Sato, Y., Furumichi, M., and Tanabe, M. (2012). KEGG for integration and interpretation of large-scale molecular data sets. Nucleic Acids Res. *40*, D109–D114.

Kubota, H., Noguchi, R., Toyoshima, Y., Ozaki, Y., Uda, S., Watanabe, K., Ogawa, W., and Kuroda, S. (2012). Temporal coding of insulin action through multiplexing of the AKT pathway. Mol. Cell *46*, 820–832.

Kühner, S., van Noort, V., Betts, M.J., Leo-Macias, A., Batisse, C., Rode, M., Yamada, T., Maier, T., Bader, S., Beltran-Alvarez, P., et al. (2009). Proteome organization in a genome-reduced bacterium. Science *326*, 1235–1240.

Li, C., Donizelli, M., Rodriguez, N., Dharuri, H., Endler, L., Chelliah, V., Li, L., He, E., Henry, A., Stefan, M.I., et al. (2010). BioModels Database: An enhanced, curated and annotated resource for published quantitative kinetic models. BMC Syst. Biol. *4*, 92.

Linding, R., Jensen, L.J., Ostheimer, G.J., van Vugt, M.A., Jørgensen, C., Miron, I.M., Diella, F., Colwill, K., Taylor, L., Elder, K., et al. (2007). Systematic discovery of in vivo phosphorylation networks. Cell *129*, 1415–1426.

Lindsay, J.R., McKillop, A.M., Mooney, M.H., Flatt, P.R., Bell, P.M., and O'harte, F.P. (2003). Meal-induced 24-hour profile of circulating glycated insulin in type 2 diabetic subjects measured by a novel radioimmunoassay. Metabolism *52*, 631–635.

Link, H., Kochanowski, K., and Sauer, U. (2013). Systematic identification of allosteric protein-metabolite interactions that control enzyme activity in vivo. Nat. Biotechnol. *31*, 357–361.

Locasale, J.W., Grassian, A.R., Melman, T., Lyssiotis, C.A., Mattaini, K.R., Bass, A.J., Heffron, G., Metallo, C.M., Muranen, T., Sharfi, H., et al. (2011). Phosphoglycerate dehydrogenase diverts glycolytic flux and contributes to oncogenesis. Nat. Genet. *43*, 869–874.

Lowery, D.M., Clauser, K.R., Hjerrild, M., Lim, D., Alexander, J., Kishi, K., Ong, S.E., Gammeltoft, S., Carr, S.A., and Yaffe, M.B. (2007). Proteomic screen defines the Polo-box domain interactome and identifies Rock2 as a Plk1 substrate. EMBO J. *26*, 2262–2273.

Miller, M.L., Jensen, L.J., Diella, F., Jørgensen, C., Tinti, M., Li, L., Hsiung, M., Parker, S.A., Bordeaux, J., Sicheritz-Ponten, T., et al. (2008). Linear motif atlas for phosphorylation-dependent signaling. Sci. Signal. *1*, ra2.

Monetti, M., Nagaraj, N., Sharma, K., and Mann, M. (2011). Large-scale phosphosite quantification in tissues by a spike-in SILAC method. Nat. Methods *8*, 655–658.

Mor, I., Cheung, E.C., and Vousden, K.H. (2011). Control of glycolysis through regulation of PFK1: old friends and recent additions. Cold Spring Harb. Symp. Quant. Biol. *76*, 211–216.

Nilsson, T., Mann, M., Aebersold, R., Yates, J.R., 3rd, Bairoch, A., and Bergeron, J.J. (2010). Mass spectrometry in high-throughput proteomics: ready for the big time. Nat. Methods *7*, 681–685.

Nimmo, H.G., and Tipton, K.F. (1975). The purification of fructose 1,6-diphosphatase from ox liver and its activation by ethylenediaminetetra-acetate. Biochem. J. *145*, 323–334.

Noguchi, R., Kubota, H., Yugi, K., Toyoshima, Y., Komori, Y., Soga, T., and Kuroda, S. (2013). The selective control of glycolysis, gluconeogenesis and glycogenesis by temporal insulin patterns. Mol. Syst. Biol. *9*, 664.

O'Connell, B.C., Adamson, B., Lydeard, J.R., Sowa, M.E., Ciccia, A., Bredemeyer, A.L., Schlabach, M., Gygi, S.P., Elledge, S.J., and Harper, J.W. (2010). A genome-wide camptothecin sensitivity screen identifies a mammalian MMS22L-NFKBIL2 complex required for genomic stability. Mol. Cell *40*, 645–657.

Oliveira, A.P., Ludwig, C., Picotti, P., Kogadeeva, M., Aebersold, R., and Sauer, U. (2012). Regulation of yeast central metabolism by enzyme phosphorylation. Mol. Syst. Biol. *8*, 623.

Olsen, J.V., Blagoev, B., Gnad, F., Macek, B., Kumar, C., Mortensen, P., and Mann, M. (2006). Global, in vivo, and site-specific phosphorylation dynamics in signaling networks. Cell *127*, 635–648.

Palsson, B. (2011). Systems biology: simulation of dynamic network states (Cambridge: Cambridge University Press).

Passonneau, J.V., and Lowry, O.H. (1963). P-Fructokinase and the control of the citric acid cycle. Biochem. Biophys. Res. Commun. *13*, 372–379.

Polonsky, K.S., Given, B.D., and Van Cauter, E. (1988). Twenty-four-hour profiles and pulsatile patterns of insulin secretion in normal and obese subjects. J. Clin. Invest. *81*, 442–448.

Rakus, D., Skalecki, K., and Dzugaj, A. (2000). Kinetic properties of pig (Sus scrofa domestica) and bovine (Bos taurus) D-fructose-1,6-bisphosphate 1-phosphohydrolase (F1,6BPase): liver-like isozymes in mammalian lung tissue. Comp. Biochem. Physiol. B Biochem. Mol. Biol. *127*, 123–134.

Rider, M.H., Bertrand, L., Vertommen, D., Michels, P.A., Rousseau, G.G., and Hue, L. (2004). 6-phosphofructo-2-kinase/fructose-2,6-bisphosphatase: head-to-head with a bifunctional enzyme that controls glycolysis. Biochem. J. *381*, 561–579.

Schomburg, I., Chang, A., Placzek, S., Söhngen, C., Rother, M., Lang, M., Munaretto, C., Ulas, S., Stelzer, M., Grote, A., et al. (2013). BRENDA in 2013: integrated reactions, kinetic data, enzyme function data, improved disease classification: new options and contents in BRENDA. Nucleic Acids Res. *41*, D764–D772.

Schöneberg, T., Kloos, M., Brüser, A., Kirchberger, J., and Sträter, N. (2013). Structure and allosteric regulation of eukaryotic 6-phosphofructokinases. Biol. Chem. *394*, 977–993.

Shyh-Chang, N., Locasale, J.W., Lyssiotis, C.A., Zheng, Y., Teo, R.Y., Ratanasirintrawoot, S., Zhang, J., Onder, T., Unternaehrer, J.J., Zhu, H., et al. (2013). Influence of threonine metabolism on S-adenosylmethionine and histone methylation. Science *339*, 222–226.

Simpson, C.J., and Fothergill-Gilmore, L.A. (1991). Isolation and sequence of a cDNA encoding human platelet phosphofructokinase. Biochem. Biophys. Res. Commun. *180*, 197–203.

Soga, T., Ueno, Y., Naraoka, H., Ohashi, Y., Tomita, M., and Nishioka, T. (2002). Simultaneous determination of anionic intermediates for Bacillus subtilis metabolic pathways by capillary electrophoresis electrospray ionization mass spectrometry. Anal. Chem. *74*, 2233–2239.

Vander Heiden, M.G., Locasale, J.W., Swanson, K.D., Sharfi, H., Heffron, G.J., Amador-Noguez, D., Christofk, H.R., Wagner, G., Rabinowitz, J.D., Asara, J.M., and Cantley, L.C. (2010). Evidence for an alternative glycolytic pathway in rapidly proliferating cells. Science *329*, 1492–1499.

Whiteman, E.L., Cho, H., and Birnbaum, M.J. (2002). Role of Akt/protein kinase B in metabolism. Trends Endocrinol. Metab. *13*, 444–451.

Wiley, H.S. (2011). Integrating multiple types of data for signaling research: challenges and opportunities. Sci. Signal. *4*, pe9.

Wittmann, C., Hans, M., van Winden, W.A., Ras, C., and Heijnen, J.J. (2005). Dynamics of intracellular metabolites of glycolysis and TCA cycle during cell-cycle-related oscillation in Saccharomyces cerevisiae. Biotechnol. Bioeng. *89*, 839–847.

Yus, E., Maier, T., Michalodimitrakis, K., van Noort, V., Yamada, T., Chen, W.H., Wodke, J.A., Güell, M., Martínez, S., Bourgeois, R., et al. (2009). Impact of genome reduction on bacterial metabolism and its regulation. Science *326*, 1263–1268.